INFECTION AND IMMUNITY, July 2004, p. 3941–3950 Vol. 72, No. 7
0019-9567/04/$08.00+0 DOI: 10.1128/IAI.72.7.3941–3950.2004

Ultrastructure of *Proteus mirabilis* Swarmer Cell Rafts and Role of Swarming in Catheter-Associated Urinary Tract Infection

Brian V. Jones, Robert Young, Eshwar Mahenthiralingam, and David J. Stickler*

Cardiff School of Biosciences, Cardiff University, Cardiff, Wales, United Kingdom CF10 3TL

Received 15 January 2004/Returned for modification 28 February 2004/Accepted 17 March 2004

Proteus mirabilis **is a common cause of catheter-associated urinary tract infection (C-UTI). It blocks indwelling urethral catheters through the formation of extensive crystalline biofilms. The obstruction of urine flow can induce episodes of pyelonephritis, septicemia, and shock. *P. mirabilis* exhibits a type of motility referred to as swarming, in which multicellular rafts of elongated, hyperflagellated swarmer cells form and move rapidly in concert over solid surfaces. It has been suggested that swarming is important in the pathogenesis of C-UTI. In this study we generated a set of stable transposon mutants deficient in swarming and used them to assess the role of swarming in the migration of *P. mirabilis* over urinary catheters. Swarming was found to be essential for migration over all-silicone catheters. Swarming-deficient mutants were attenuated in migration over hydrogel-coated latex catheters, but those capable of swimming motility were able to move over and infect these surfaces. A novel vapor fixation technique for the preparation of specimens and scanning electron microscopy were used to resolve the ultrastructure of *P. mirabilis* multicellular rafts. The flagellar filaments of *P. mirabilis* were found to be highly organized during raft migration and were interwoven in phase to form helical connections between adjacent swarmer cells. Mutants lacking these novel organized structures failed to swarm successfully. We suggest that these structures are important for migration and formation of multicellular rafts. In addition, the highly organized structure of multicellular rafts enables *P. mirabilis* to initiate C-UTI by migration over catheter surfaces from the urethral meatus into the bladder.**

Indwelling bladder catheterization is a convenient way to manage the problems of urinary retention and incontinence that afflict so many elderly and disabled people. The catheter, however, forms a bridge along which bacteria can pass from a contaminated external environment into a vulnerable body cavity. Even with meticulous nursing care, all patients undergoing catheterization for longer than a month will develop urinary tract infections (16). The number of catheterized patients is so large that catheter-associated urinary tract infections (C-UTI) are the most common infections acquired in hospitals and other health care facilities (29).

Proteus mirabilis poses particular problems in the care of patients undergoing long-term indwelling bladder catheterization. Infections with this organism result in the formation of extensive crystalline biofilms on the catheters that can block the flow of urine from the bladder (28). The crystalline material, composed of magnesium and calcium phosphates, precipitates out of solution under the alkaline conditions generated by the *P. mirabilis* urease enzyme (5, 13, 20). The obstruction of the flow of urine through the catheter can induce serious complications. Urine either leaks around the outside of the catheter causing patients to become incontinent or is retained in the bladder resulting in painful distension of the bladder and reflux of urine to the kidneys, which can initiate episodes of pyelonephritis, septicemia, and shock (16). It has been suggested that the well-known ability of *P. mirabilis* to swarm rapidly over surfaces may play a role in the pathogenicity of this species in the catheterized urinary tract (4). Swarming is a cyclic, multicellular behavior allowing rapid migration of "rafts" of *P. mirabilis* cells over solid surfaces. On contact with a solid surface, *P. mirabilis* swimmer cells (1 to 2 μm in length) differentiate into elongated, hyperflagellated swarmer cells (up to 80 μm long), which exhibit increased expression of virulence factors (3, 4).

Several clinical studies have indicated that bacteria may gain access to the bladder by migration along the external surfaces of the catheter (10, 26). Using a simple laboratory model, Stickler and Hughes (27) demonstrated that *P. mirabilis* could swarm rapidly over all of the major types of catheter and suggested that swarming may play a role in both the initiation of *P. mirabilis* C-UTI and the subsequent spreading of the biofilm over the catheter surface.

The aim of this study was to explore further the hypothesis that *P. mirabilis* C-UTI may be initiated by the migration of rafts of swarmer cells over catheter surfaces. A collection of swarming-deficient mutants was generated by random transposon-based mutagenesis. These mutants were characterized phenotypically by electron microscopy, and their ability to migrate over the surfaces of urethral catheters was examined.

MATERIALS AND METHODS

Bacterial strains and culture. *P. mirabilis* strain B4, a recent clinical isolate from an encrusted indwelling urethral catheter, was used as the test strain in this study. Identification of strain B4 and all derivative mutants was confirmed with a BBL crystal enteric/nonfermenter ID system (Becton Dickinson, Oxford, United Kingdom). Bacteria were grown on Luria-Bertani (LB) medium (25) at 37°C. Bacteriological agar and the constituents of LB medium were purchased from Oxoid, Basingstoke, United Kingdom. Standard LB medium containing 1.5% agar (LB agar) was used for general growth of strain B4 and derived mutants, LB medium containing 0.7% agar (soft LB agar) was used for swarming mutant isolation, and LB medium containing 0.3% agar (motility LB agar) was used to evaluate *P. mirabilis* swimming ability. MacConkey agar (Oxoid) without

* Corresponding author. Mailing address: Cardiff School of Biosciences, Cardiff University, Main Bldg., Rm. 1.53, Cardiff, Wales, United Kingdom CF10 3TL. Phone: 44 2920874311. Fax: 44 2920874305. E-mail: Stickler@Cardiff.ac.uk.

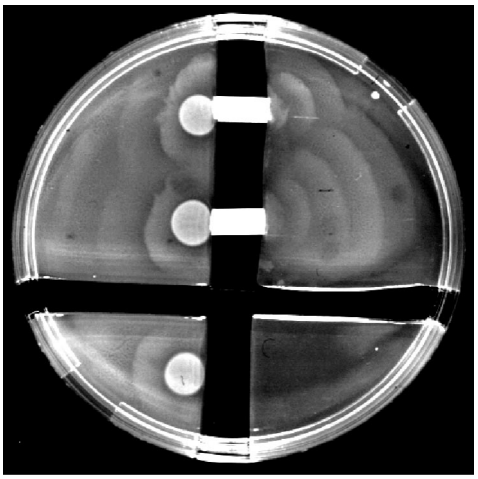

FIG. 1. *P. mirabilis* migrating over 1-cm sections of hydrogel-coated latex catheter.

salt was used for isolation of single colonies of *P. mirabilis*. The antimicrobial agents kanamycin (30 μg/ml), polymyxin (60 U/ml), and ampicillin (100 μg/ml) were added to growth media as appropriate.

Random transposon mutagenesis of *P. mirabilis* strain B4. Swarming-deficient mutants were generated from *P. mirabilis* strain B4 with a mini-Tn*5*Km2 transposon and the pUT suicide delivery vector (7). The delivery vector pUT, carrying mini-Tn*5*Km2, was transferred to *P. mirabilis* strain B4 from the *Escherichia coli* S17.1λ*pir* donor strain by conjugation as described by Lewenza et al. (17). Transconjugant *P. mirabilis* colonies were selected on MacConkey agar supplemented with kanamycin (30 μg/ml) and polymyxin (60 U/ml). All transposon mutants were subsequently cultured on media containing kanamycin (30 μg/ml).

Isolation of swarming-deficient mutants. Mutants defective in swarming were isolated by screening 1,000 *P. mirabilis* transconjugants for inability to spread beyond the point of inoculation over soft LB agar. Isolated mutants were then subcultured on standard LB agar. Loss of the pUT delivery vector was verified by sensitivity to ampicillin. Transconjugant strains were confirmed as *P. mirabilis*, and the presence of single random mini-Tn*5*Km2 inserts was verified by Southern hybridization with a digoxigenin (DIG)-labeled mini-Tn*5*Km2-specific probe. Probes were generated by PCR amplification of the mini-Tn*5*Km2 *nptII* gene with DIG-labeled deoxynucleoside triphosphates (Roche, Lewes, United Kingdom) and primers NPT2_F1 (5′-CTTGCTCGAGGCCGCGATTAAATT-3′) and NPT2_R1 (5′-TTCCATAGGATGGCAAGATCCTGG-3′). Probe hybridization was performed in accordance with standard protocols (25). Probe detection was accomplished with an antibody-based chemiluminescence detection kit (DIG luminescence detection kit for nucleic acids; Roche) in accordance with the manufacturer's instructions.

Genetic characterization of transposon mutants. Analysis of transposon insertions was performed by (i) subcloning and sequence analysis exactly as described by de Lorenzo and Timmis (7) and (ii) direct PCR sequence analysis of DNA flanking the transposon insertion as described by Manoil (18). The sequence at the transposon insertion junction was correlated with the *P. mirabilis* strain HI4320 genome project. Genome data were produced by the Pathogen Sequencing Group at the Sanger Institute, Hinxton, Cambridge, United Kingdom, and can be obtained at http://www.sanger.ac.uk/Projects/P_mirabilis/. Bioinformatic analysis and annotation were performed with the Artemis software (http://www.sanger.ac.uk/Software/Artemis/) and the basic local alignment search tool at the National Center for Biotechnology Information website (http://www.ncbi.nlm.nih.gov/index.htm). Protein family information was obtained from the Protein Families databases of Alignments and HMMs (http://www.sanger.ac.uk/Software/Pfam/index.shtml) and the Clusters of Orthologous Groups database (http://www.ncbi.nlm.nih.gov/COG/).

Assessment of swimming and swarming activities. Swarming motility was characterized on dry LB agar plates. A 10-μl drop of an overnight culture was inoculated onto the center of each plate. The drops were allowed to soak into the agar at room temperature, and then the plates were incubated for 8 h at 37°C. To assess swimming motility, 2-μl drops of an overnight culture were stabbed into the center of motility LB agar plates, and then the plates were incubated for 6 h at 37°C. The distance migrated on both types of agar from the point of inoculation was measured. The swimming and swarming abilities of each mutant were expressed as percentages of those of the wild type to produce swarming and swimming indices for each mutant.

Migration of *P. mirabilis* over urethral catheters. The ability of the swarming-deficient mutants to migrate over the surfaces of urethral catheters was assessed by the catheter bridge model described by Stickler and Hughes (27). Plates of standard LB agar were dried, and 0.8-cm-wide channels were cut across their centers. Aliquots (10 μl) of 4-h cultures of test strains grown in LB broth were inoculated at the edge of the channel. After the inocula had dried into the agar, sections (1 cm) of all silicone or hydrogel-coated latex catheters (Bard, Crawley, United Kingdom) were placed as bridges between the agar blocks, adjacent to points of inoculation. As a control, one point of inoculation on each plate was not provided with a catheter bridge, and the corresponding area of the opposing agar block was isolated by a 0.5-cm channel (Fig. 1). Plates were incubated at 37°C for 24 h, and migration across catheter sections was identified by growth on the uninoculated halves of the plate, adjacent to catheter bridges. Each mutant was

TABLE 1. Assessment of swarming and swimming abilities of *P. mirabilis* B4 and transposon mutants

Group	Strain	Agar swarming index[a]	Agar swimming index[a]	Catheter bridge migration index[b]	
				All silicone	Hydrogel-coated latex
Wild type	B4	100	100	66.67	100
1, Control mutants	BVJ14	167.8	100	41.67	100
	BVJ12	110.1	100	41.67	100
	BVJ15	105	95.5	16.67	100
2, Poor-swarming mutants	NS77	16.95	74.6	16.67	58.33
	G77	15.25	86.1	0	75
	PS92	10.17	106.1	0	75
	G78	0	36.9	8.33	58.33
	G64	0	28.5	0	58.33
3, Nonswarming mutants	G93	0	42.30	0	66.67
	G37	0	40	0	50
	G33	0	32.3	0	33.3
4, Nonswimming, nonswarming mutants	NS63	0	0	0	0

[a] Swimming and swarming indices are expressed as percentages of those of the wild type as described in Materials and Methods.
[b] The migration index was calculated as the percentage of catheter bridges crossed by each strain in 12 replicate experiments.

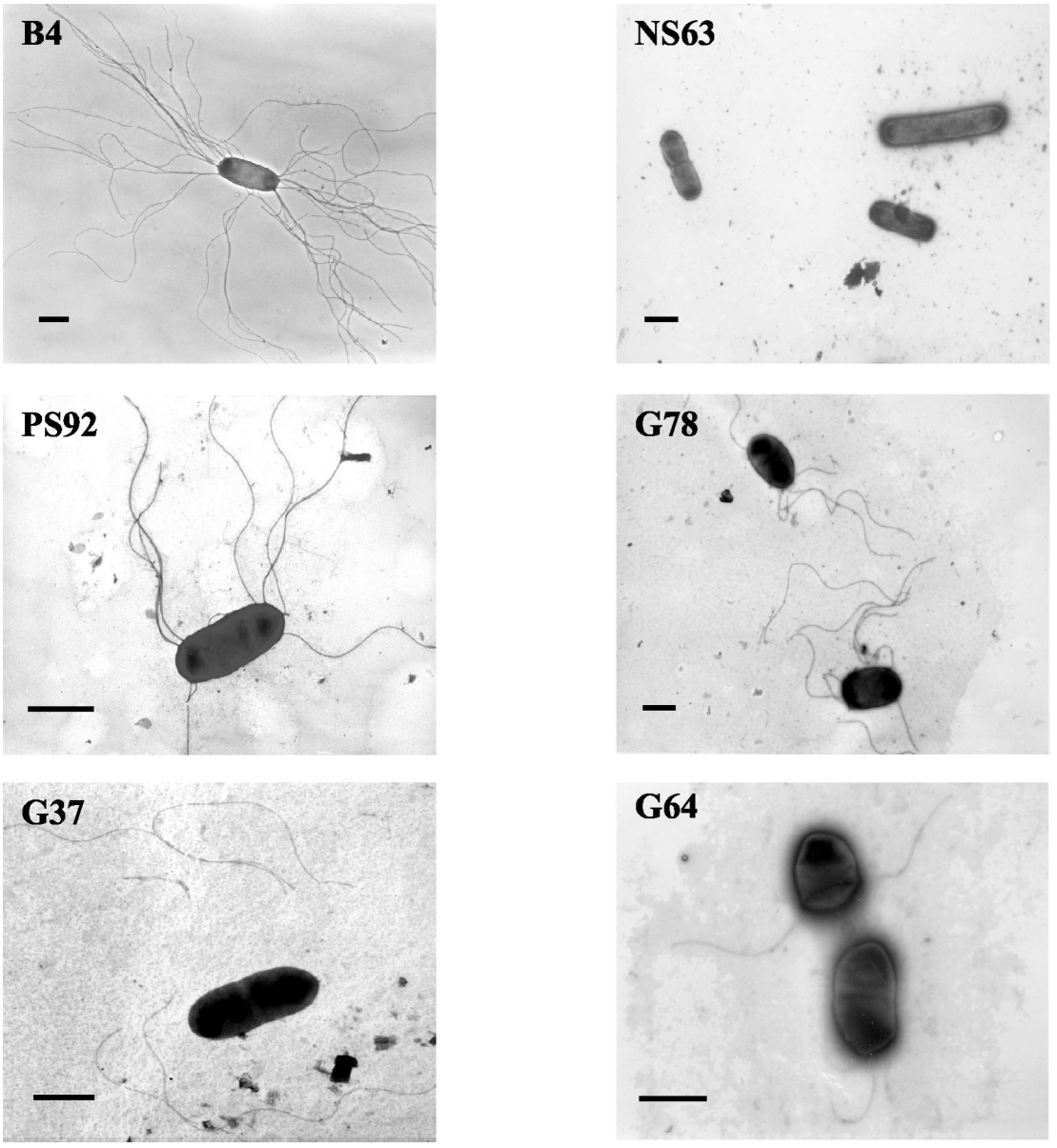

FIG. 2. TEM observations of wild-type *P. mirabilis* and transposon mutants illustrating differences in flagellar production and phenotype. Strains: B4, wild type; PS92, poor-swarming mutant; NS63, nonswarming, nonswimming mutant; G78, poor-swarming mutant; G37, nonswarming mutant; G64, poor-swarming mutant. Bars = ~1 μm.

tested on 12 replicate catheter sections, and a migration index was calculated as the percentage of these bridges crossed.

Demonstration of flagella in swimming cells. Flagella of wild-type and mutant *P. mirabilis* were visualized by negative staining of swimmer cells and examination by transmission electron microscopy (TEM). Strains were grown in LB broth overnight at 37°C with aeration. Formvar-coated copper grids were floated on a drop of an overnight culture for 1 min. Grids were then washed three times by floating on drops of sterile deionized water for 30 s. Finally, cells were negatively stained by floating the grids on a drop of 1% uranyl acetate for 1 min. Samples were then viewed with a Philips TEM208 transmission electron microscope.

Scanning electron microscopy (SEM) of swarm fronts. Swarm fronts of mutant and wild-type *P. mirabilis* were fixed in situ on LB agar by vapor fixation. *P. mirabilis* strain B4 was grown in LB broth, while mutant strains were cultured in LB broth supplemented with kanamycin. Cultures were incubated overnight at 37°C with aeration. Aliquots (10 μl) of overnight cultures of test strains were inoculated onto the centers of the LB agar plates and incubated at 37°C to allow swarming. Plates were removed during active migration of swarm fronts and suspended face down over 10 ml of an aqueous solution containing 12.5% electron microscopy grade glutaraldehyde (Agar Scientific, Stanstead, United Kingdom) and 8% paraformaldehyde (Agar Scientific) in a sealed staining dish for 18 to 24 h at room temperature. After vapor fixation, blocks of agar (1 cm^2) supporting a section of the swarm front were cut from the plates with a sterile scalpel. Blocks were stained by immersion in aqueous osmium tetroxide (1%, wt/vol; Agar Scientific) for 1 h and dehydrated in a series of ethanol solutions (70, 90, and 2 × 100%) before critical-point drying. The dehydrated blocks were then sputter coated with gold, and swarm fronts were viewed with a Philips XL20 scanning electron microscope.

TEM of swarm fronts. Swarm fronts of *P. mirabilis* strain B4 were prepared by in situ vapor fixation as for SEM observations. The agar blocks supporting swarm fronts were postfixed by immersion in aqueous osmium tetroxide (1%, wt/vol) and then dehydrated in a series of ethanols (70, 90, and 2 × 100%). Dehydrated blocks were "cleared" by immersion in propylene oxide twice for 15 min and infiltrated with Araldite embedding resin for 30 h by agitation at room temperature. Blocks were then embedded in resin, which was polymerized by incubation

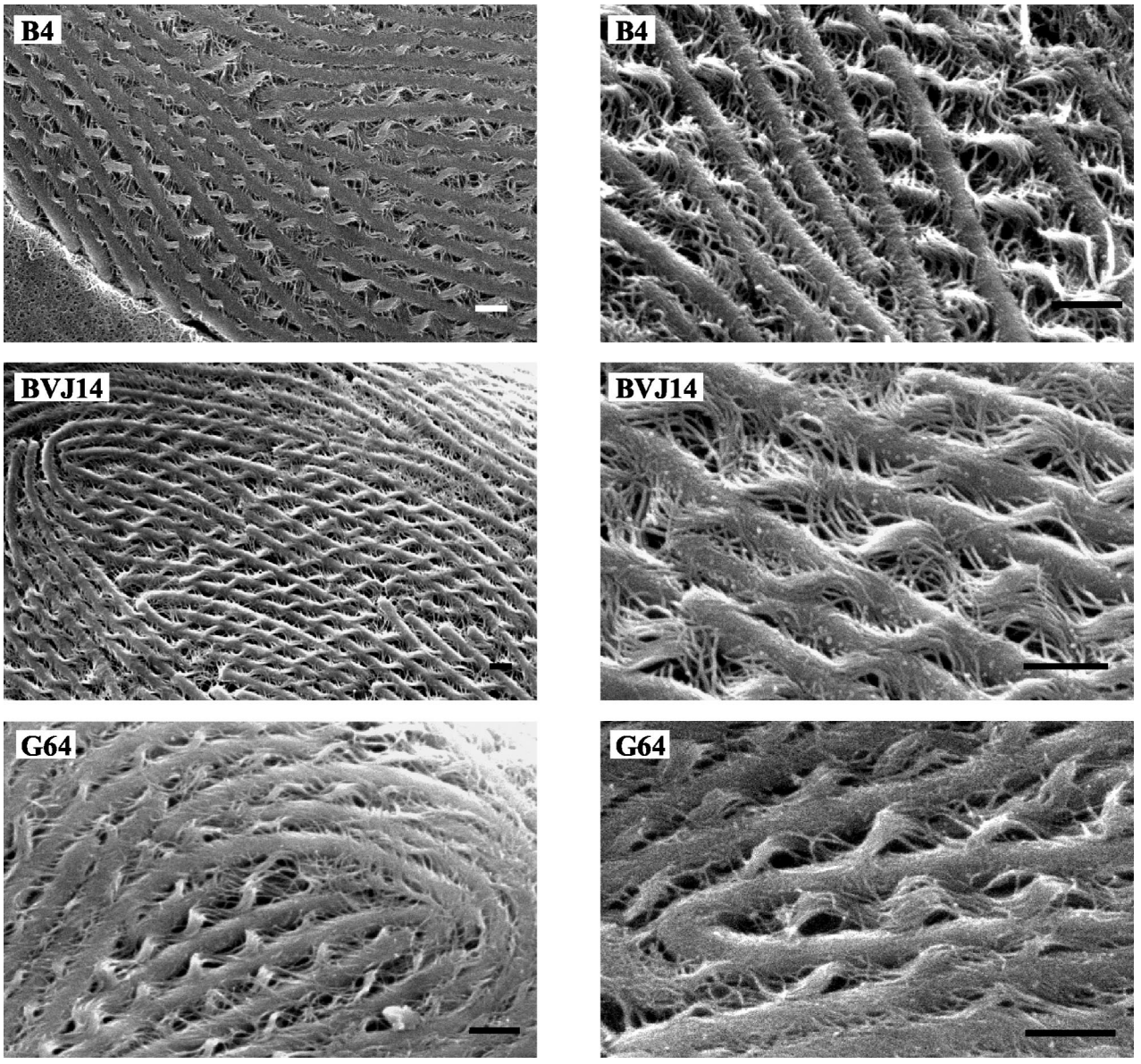

FIG. 3. SEM of in situ vapor-fixed swarm fronts of wild-type *P. mirabilis* and transposon mutants exhibiting helical connections. Strains: B4, wild type, BVJ14, transposon-containing control mutant, G64, poor-swarming mutant. Bars = ~1 μm.

at 60°C for 24 h. Thin sections (80 nm thick) were cut from embedded blocks with a Reichart Ultracut microtome and diamond knife. The thin sections were collected on uncoated copper grids and stained by immersion in aqueous uranyl acetate (2%, wt/vol) for 10 min and then in Reynolds's lead citrate for 5 min. Samples were viewed with a Philips TEM208 transmission electron microscope.

RESULTS

Isolation of swarming-deficient mutants. A total of 1,000 random transposon mutants of *P. mirabilis* B4 were screened, and 150 mutants with alterations in the swarming phenotype were identified. Nine stable transposon mutants deficient in swarming and possessing single mini-Tn*5*Km2 inserts at discreet loci (data not shown) were selected for further analysis. In addition, three stable transposon mutants that demonstrated no alterations in swarming were included as controls to assess possible adverse effects of the presence of the transposon on swarming. The abilities of these 12 strains and parent strain B4 to swarm over and swim through LB agar were tested. The swimming and swarming indices of each mutant and the control strain are shown in Table 1. The 12 stable mutants were divided into four categories, based on their swarming and swimming indices on agar, which consisted of mutants unaffected in swarming (group 1), poor-swarming mutants (group 2), nonswarming mutants (group 3), and mutants that failed to swim or swarm (group 4). Mutants G64 and G78 did not initiate swarming during the swarming assay and produced a swarming index of 0 (Table 1). However, after overnight incubation both mutants exhibited swarming and were therefore classified as poor-swarming mutants (group 2).

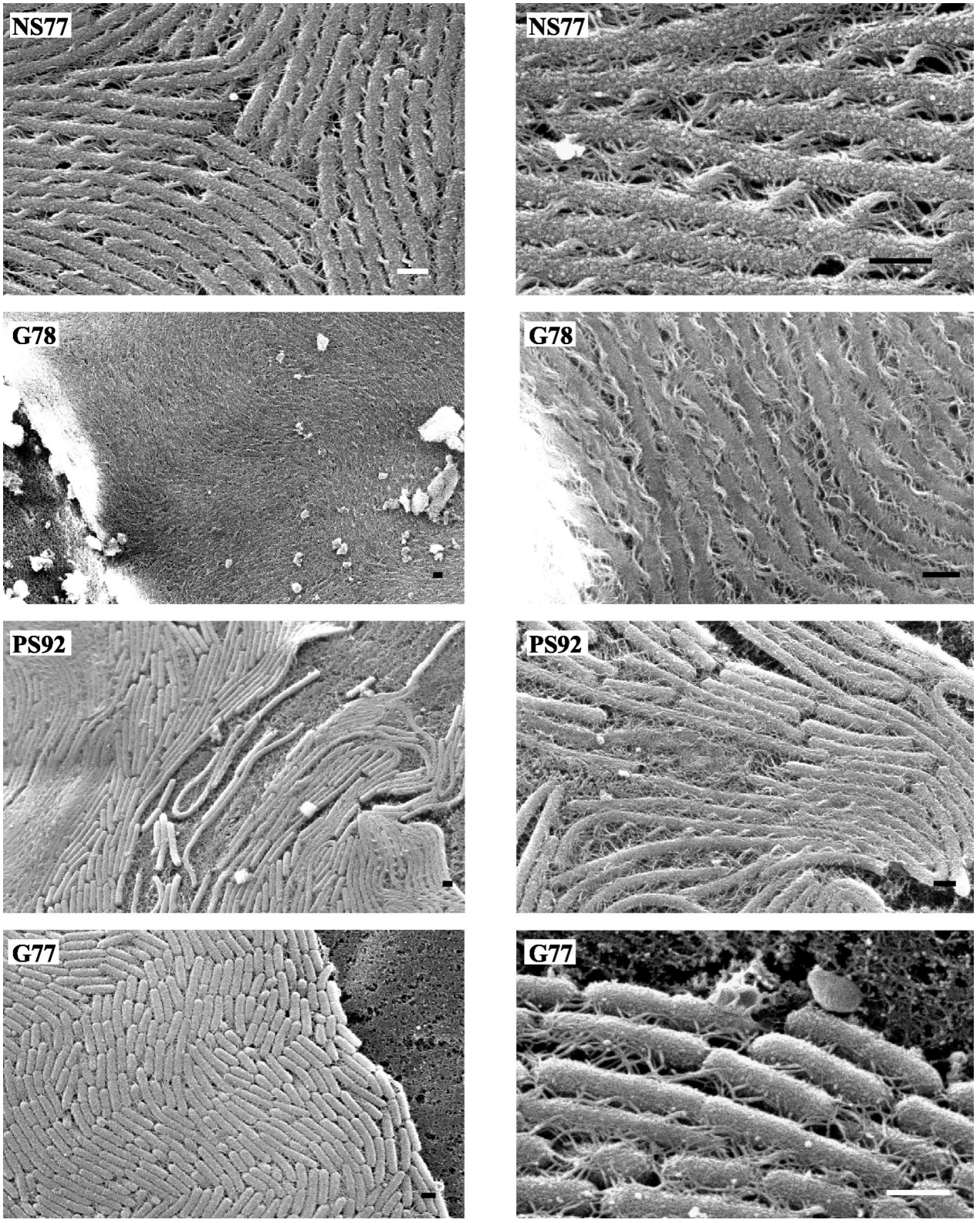

FIG. 4. SEM observations of in situ vapor-fixed swarm fronts of poor-swarming mutants exhibiting abnormal helical connections. Bars = ~1 μm.

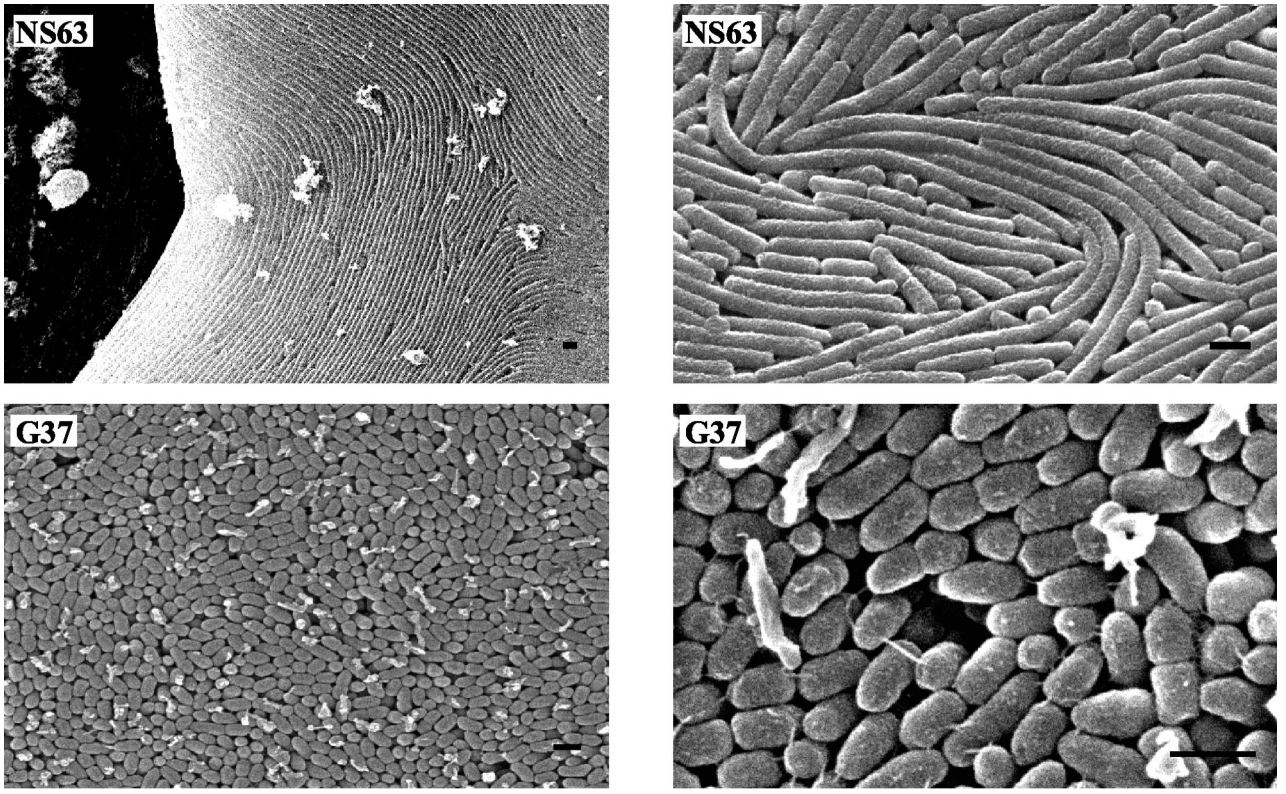

FIG. 5. SEM observations of in situ vapor-fixed swarm fronts of nonswarming mutants that do not produce helical connections. Bars = ~1 μm.

Demonstration of flagella in swimming cells. TEM was performed on LB broth cultures of the wild type and 12 transposon mutants (Table 1), and selected micrographs are presented in Fig. 2. Wild-type strain B4 typically produced approximately 30 long (~10 to 12 μm) flagella per cell. The control mutants (such as BVJ14), which harbor the mini-Tn*5*Km2 transposon but are capable of swarming, produced similar numbers of normally shaped flagella. All mutants deficient in swarming (such as PS92) produced fewer flagella (0 to 11) than the wild type, and several appeared to produce abnormal flagella. The defects observed included alterations in flagellar shape (G78, Fig. 2), decreased length of flagella (G64, Fig. 2), and dissociation of flagellar filaments from cells (G37, Fig. 2). No flagella were observed on nonswarming, nonswimming mutant NS63 (Fig. 2).

SEM of swarm fronts. Swarm fronts of the wild type and mutants were observed by SEM. Swarm fronts were fixed in situ, during active migration on agar, by vapor fixation. Wild-type strain B4 and the control mutants (such as BVJ14) were aligned to form multicellular rafts of parallel cells (Fig. 3). Cells at the swarm front were elongated and hyperflagellated (Fig. 3), which is consistent with previous observations of *P. mirabilis* swarmer cells (2, 4, 12). However, in situ vapor fixation revealed a completely novel aspect of the *P. mirabilis* swarming cycle. Observations of the wild type and control mutants showed that the flagellar filaments of *P. mirabilis* are highly organized during migration and appear to be interwoven in phase to form helical connections between adjacent swarmer cells (Fig. 3).

The poor-swarming mutant G64 (Table 1, group 2) also exhibited helical connections (Fig. 3), but these structures were less evident in all other poor-swarming mutants (Table 1, group 2), and flagellar filaments appeared less organized (Fig. 4). Helical connections were not observed on the nonswarming mutants (such as G37 and NS63) (Fig. 5). Nonswarming mutants G33, G37, and G93 did not form the elongated, hyperflagellated swarmer cells seen in the wild type (Fig. 5). Nonswarming mutant NS63, however, retained the ability to produce elongated cells (Fig. 5). A summary of the observations on the swarm fronts of all strains is presented in Table 2.

TEM of B4 swarm fronts. The nature of flagellar organization during migration of swarmer cells was also investigated by TEM. Thin sections cut through wild-type swarm fronts fixed in situ during active migration on agar were observed. Micrographs of both transverse and longitudinal sections are presented in Fig. 6. The transverse sections confirmed that flagellar filaments were tightly interwoven during migration and are localized between adjacent cells in the monolayer of swarmer cells (Fig. 6). Observations of the longitudinal sections revealed that the flagellar filaments are interwoven in a crisscross pattern (Fig. 6).

Migration of *P. mirabilis* over the surfaces of urinary catheters. The abilities of the test strains to migrate over the surfaces of sections of all-silicone and hydrogel-coated latex catheters were examined. These experiments showed that migration occurred more readily over hydrogel-coated latex sections than over all-silicone sections (Table 1). The migration indices of the swarming-deficient mutants were all lower

TABLE 2. Summary of SEM observations of swarm fronts of wild-type *P. mirabilis* and transposon mutants

Group	Strain	Organisation of flagellar filaments	Cellular organization at swarm fronts	Figure
Wild type and 1 (control mutants)	B4	Flagellar filaments localized between adjacent cells and interwoven to form regular helical connections	Cells elongated, similar in length, and organized into rafts of parallel swarmer cells	3
	BVJ14			
	BVJ12			
	BVJ15			
2, Poor-swarming mutants	NS77	Helical connections formed but composed of fewer flagellar filaments than those observed in wild type	Same as wild type	4
	G77	Evidence of vestigial helical connections but flagellar organization greatly reduced	Cells lack organization seen in wild-type swarm fronts; cell length reduced	4
	PS92	Helical connections formed but not uniformly throughout swarm front	Large variation in cell length at swarm front; cells formed poorly organized rafts and were unable to maintain formation	4
	G78	Flagellar filaments organized and interwoven but do not form a regular helical pattern	Cells organized into rafts but were closer together than cells in wild-type swarm fronts	4
	G64	Same as wild type	Same as wild type	3
3, Nonswarming mutants	G37	No helical connections formed but some short flagellar filaments visible	No elongation or cellular organization	5
	G33	No helical connections formed, no visible flagellar filaments	Cells exhibit slight elongation, have a mucoid appearance, and show some alignment	
	G93	No helical connections formed but some flagellar filaments visible	Cells exhibit slight elongation and some alignment at the colony boundary	
4, Nonswimming, nonswarming mutants	NS63	No helical connections formed, no visible flagellar filaments	Large variation in cell length with some extensively elongated cells; elongated cells appear to align	5

than that of the wild type. Swarming-deficient mutants were less able to migrate over the surfaces of both types of catheter. Nonswarming mutants were unable to migrate over all-silicone catheters, but those capable of swimming were able to migrate over hydrogel-coated latex catheters. Nonswarming, nonswimming mutant NS63 failed to migrate over any of the catheter sections.

Identification of transposon-disrupted genes. The point of transposon insertion was determined for one mutant from each swarming and swimming class (Table 1). The genetic basis for mutants BVJ14, G77, G93, and NS63 is presented in Table 3. The *P. mirabilis* strain B4 DNA sequence at the transposon junction correlated exactly with the genome sequence of strain HI4320 and produced significant homology to known coding sequences (CDS) for all four of the latter mutants. Control mutant BVJ14 was disrupted in an outer membrane protein CDS with homology to those found in colicin receptor systems. Poor-swarming mutant G77 possessed an intergenic disruption between a transcriptional regulator and a chemotaxis-related CDS, both of which could play a role in swarming. The transposon insertion in nonswarming mutant G93 disrupted a *surA*-like CDS implicated in protein posttranslational modification-turnover and chaperone functions (Table 3). Finally, the nonswimming, nonswarming mutant contained a transposon insertion in a gene homologous to *flhA*, a component of the flagellar regulon that has been shown to be essential for *P. mirabilis* motility and swarming (12).

DISCUSSION

Few studies have investigated the migration of bacteria over catheter surfaces. Darouiche et al. (6) reported that of four bacterial species tested, *Pseudomonas aeruginosa* was the most mobile in a model of bladder colonization, where it took 12 days to migrate along a 10-cm length of all-silicone catheter. In view of its importance as a pathogen of the catheterized urinary tract, it was surprising that *P. mirabilis* was omitted from that study. Sabbuba et al. (24) demonstrated that *P. mirabilis* and *P. vulgaris* swarmer cells migrated more successfully over all-silicone catheter sections than did nine other urinary tract pathogens, including *P. aeruginosa*. Previous work by our group has demonstrated that *P. mirabilis* can swarm over a variety of urethral catheters (27). We undertook the present study to systematically assess the role of swarming in the initiation of C-UTI by *P. mirabilis* and examine the ultrastructure of multicellular rafts of swarmer cells in situ during active migration.

By investigating the swarming and swimming abilities of the stable transposon mutants generated in this study, we revealed four classes of mutants (Table 1). The control mutants (Table 1, group 1) showed that the presence of the mini-Tn*5*Km2

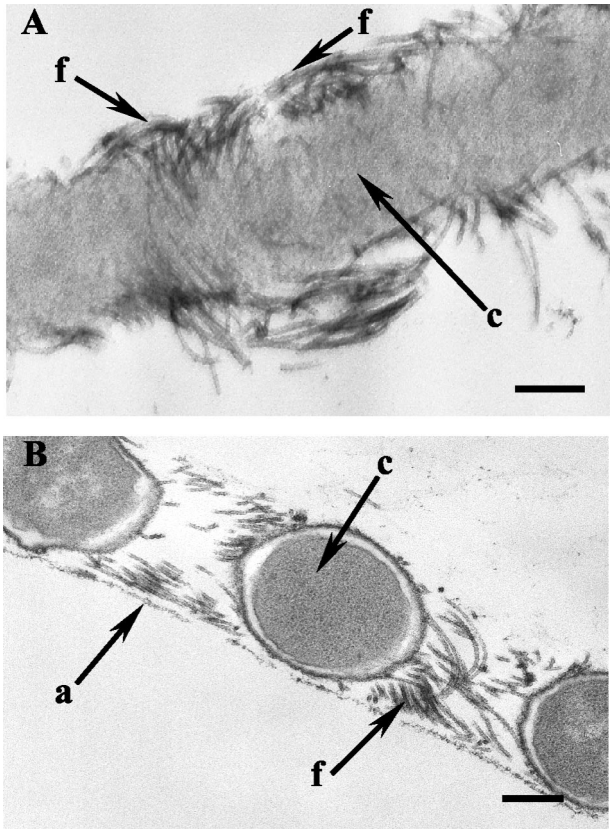

FIG. 6. TEM observation of a longitudinal section (A) and a transverse section (B) through a wild-type swarm front during migration over agar. The swarm front was fixed in situ by vapor fixation. Arrows indicate flagellar filaments (f), the agar surface (a), and cells (c). The longitudinal section (A) shows flagellar filaments interweaving with and against the direction of migration. The transverse section (B) shows that flagellar filaments are mainly localized between adjacent cells during migration. Bars = ~300 nm.

transposon in the host chromosome per se did not impair the swarming or swimming ability of the mutants. In addition, TEM observation of swimmer cells in LB broth culture (Fig. 2) revealed that flagellar production was also unaffected in these mutants. With the exception of PS92, all of the swarming-deficient mutants showed decreased swimming ability compared to that of the wild type (Table 1). Of the poor-swarming mutants, those with the lowest swarming indices (G64 and G78) also possessed the lowest swimming indices (Table 1, group 2).

It seems probable that the altered flagella produced by G78 (altered flagellar shape), G64 (decreased length of flagella), and G37 (flagellar filaments dissociated from the cell) account for the poor swimming ability of these mutants (Fig. 2). Kanto et al. (14) reported that *Salmonella enterica* serovar Typhimurium mutants that produced flagella abnormal in shape were unable to swim normally. It has been suggested that the flagella themselves may contribute significantly to the pathogenicity of *P. mirabilis* (19), and flagellar synthesis and swimming motility have been identified as important processes in the formation of biofilms of *P. aeruginosa* and *E. coli* (21, 22). Flagella are also key structures in *P. mirabilis* swarming (4, 8, 11, 12). The flagellar filaments of *P. mirabilis* are thought to act as tactile sensors allowing the cell to sense contact with solid surfaces (4). It has been suggested that inhibition of flagellar rotation due to increased viscosity of the medium or contact with solid surfaces triggers swarmer cell differentiation in *P. mirabilis* (4).

P. mirabilis mutants unable to synthesize flagella were found not only to be nonmotile but to be unable to differentiate into elongated swarmer cells (4, 12). In addition, *P. mirabilis* mutants unable to produce flagella were attenuated in virulence in murine models of urinary tract infection (1, 19). Flagella were not observed on nonswimming, nonswarming mutant NS63 (Fig. 2). Interestingly, SEM observations of NS63, in situ on agar, revealed that this mutant had retained the ability to generate elongated cells (Fig. 5). Characterization of the disrupted locus in this novel class of mutant may provide a greater understanding of swarm cell differentiation in *P. mirabilis*. Fraser et al. (9) suggested that a threshold number of flagella are required before differentiation and swarming of *P. mirabilis* can occur. TEM observations of all swarming-deficient mutants revealed a decrease in flagellar production (Fig. 2). SEM observations of nonswarming mutants G33, G37, and G93 showed that they are unable to differentiate normally (Fig. 5). Poor-swarming mutants, however, also showed low levels of flagellar production compared to the wild type but were still able to differentiate and swarm (Fig. 4). The inability of G37 to differentiate (Fig. 5) may also be related to the dissociation of flagellar filaments from the cell observed in this mutant (Fig. 2). This defect in flagellar production may impede the ability of G37 to sense contact with a solid surface and initiate differentiation.

The role of flagella in *P. mirabilis* swarm cell differentiation has been well studied. In contrast, the mechanisms underlying the flagellum-driven migration of multicellular rafts of swarm cells has received little attention. In this study, a new vapor fixation method for specimen preparation and SEM were used to observe swarm fronts during migration on 1.5% LB agar. This permitted the resolution of novel structures involved in multicellular raft formation and migration of *P. mirabilis* (Fig. 3 and Table 2). These structures were termed helical connections and were formed by the interweaving of flagellar filaments from adjacent swarmer cells. To our knowledge, this is the first report of this aspect of the *P. mirabilis* swarming cycle. Lateral flagella of swarming *Aeromonas* species have also been found to form linkages between individual cells on an agar surface (15), but the formation of helical connections between *P. mirabilis* swarmer cells appears to be a far more ordered process. TEM observations of thin sections cut through wild-type swarm fronts (Fig. 6), along with the highly ordered structure of helical connections observed by SEM (Fig. 3), suggest a process of active organization in which flagellar filaments are arranged into these specific formations.

The formation of helical connections may contribute to the stability of multicellular rafts. Poor-swarming mutant PS92 possesses the ability to form helical connections but does not generate them uniformly throughout the swarm front. PS92 rafts appear to lack cohesion, and cellular organization is not maintained. Studies of the multicellular behavior of *S. enterica* serovar Typhimurium indicate that flagella play a similar role in pellicle formation by this organism, holding clumps of cells

TABLE 3. Genetic basis of *P. mirabilis* transposon mutants

Group, transposon mutant	*P. mirabilis* DNA sequence at transposon junction (5′ to 3′)[a]	Putative identity of disrupted genetic locus
1, Control mutant BVJ14	CTTTAGTGGTTGCAAACTCA	*cirA*-like CDS for an outer membrane receptor for colicin uptake (COG1629)
2, Poor-swarming mutant G77	CTAATGTCCACAGTATTAAG	Intergenic mutation between *acrR*-like transcriptional regulator CDS (COG1309) and methyl-accepting chemotaxis protein CDS (pfam00015)
3, Nonswarming mutant G93	GTGTAGACCAACACCTGATT	*surA*-like CDS for a parvulin-like peptidyl-prolyl isomerase (COG0760)
4, Nonswimming, nonswarming mutant NS63	GTGTTACATAAAGTATTGCA	*flhA* homologue part of flagellar biosynthesis pathway (COG1298)

[a] The disrupted locus for each mutant may be obtained by matching each sequence to the *P. mirabilis* genome project as described in Materials and Methods.

together (23). Communication between swarmer cells may also be facilitated by the formation of helical connections. These structures could hold swarmer cells at the optimum distance for, or play a more direct role in, intercellular communication. Linking of flagellar filaments through the formation of helical connections could form a network of tactile sensors and may allow cells to coordinate certain aspects of the swarming cycle, such as migration velocity and direction.

The organization of flagellar filaments into these structures may also play an important role in the migration of multicellular rafts. Formation of helical connections could serve to coordinate flagellar rotation in order to generate sufficient force for propulsion of these rafts. SEM observations of the swarming-deficient mutants showed that all poor-swarming mutants, with the exception of G64 (Fig. 3), exhibited defects in the production of helical connections (Fig. 4), and these structures were not found in nonswarming mutants (Fig. 5). The coordination of flagella would be particularly important for movement over surfaces exigent to migration, including some catheter biomaterials such as silicone.

The results of the catheter bridge experiments (Table 1) confirm the observations of Stickler and Hughes (27) that *P. mirabilis* migrates more easily over the surfaces of hydrogel-coated latex catheters than over those of all-silicone catheters. It is also clear that the nonswarming mutants failed completely to cross all-silicone sections, but those that had retained the ability to swim were able to migrate over hydrogel-coated latex sections. Nonswimming, nonswarming mutant NS63 failed to cross any catheter sections. Overall, swarming is important for *P. mirabilis* migration over the tested catheter surfaces. Swarming was essential for migration over all-silicone catheter sections. Swarming-deficient mutants were attenuated in migration over hydrogel-coated latex catheters, but those capable of swimming motility were able to move over these catheter sections. Similar conclusions were drawn by Sabbuba et al. (24) from catheter bridge experiments performed under conditions that inhibited the formation of *P. mirabilis* swarmer cells.

The genetic basis of four of the *P. mirabilis* transposon mutants was determined and correlated with their phenotypic features (Table 3). The colicin receptor mutation in control mutant BVJ14 would be expected to be relatively unrelated to genes implicated in swarming or swimming motility. However, all three of the swarming- or swimming-deficient mutants evaluated possessed plausible genotypes. The intergenic transposon disruption in poor-swarming mutant G77 may have altered the expression of either a transcriptional regulator CDS or a chemotaxis-related CDS, both of which could play an active role in swarming. The *surA* mutation in nonswarming mutant G93 may have significantly altered protein modification, turnover, and targeting. Since swarming triggers the expression of a large number of proteins that have to be targeted to a variety of different cellular locations, it is logical that proteins such as SurA that are implicated in modification or chaperonin functions would play a significant role in this differentiation process (Table 3).

The identification of *flhA* as the genetic basis for nonswimming, nonswarming mutant NS63 is clearly linked to the phenotype of this *P. mirabilis* transposon mutant. FlhA is an essential flagellar component and has been shown to be required for both flagellar assembly and swarm cell differentiation in *P. mirabilis* (12). Mutant NS63 was the only strain that was incapable of crossing both all-silicone and hydrogel-coated catheter bridges (Table 1). To demonstrate that *flhA* plays a functional role in this infection process, mutant NS63 was complemented with the corresponding wild-type *P. mirabilis* strain B4 locus (B. Jones, unpublished data). Swimming and swarming were restored in the complemented mutant, and it was capable of crossing both types of catheter. The same plasmid construct was also shown to complement the motility of a known *flhA* mutant of *P. mirabilis* strain U6450 (12), confirming that the genetic basis of transposon mutant NS63 correlated with its motility-deficient phenotype.

In conclusion, the vapor fixation technique has revealed that rafts of *P. mirabilis* swarmer cells are held together by large numbers of flagellar filaments interwoven in phase to form helical connections between adjacent swarmer cells. Initial studies also indicate that these structures may play a role in the migration of these rafts over solid surfaces. Mutants lacking helical connections failed to swarm successfully. The catheter bridge experiments suggest that, at least in the case of all-silicone catheters, swarming could be involved in the migration of *P. mirabilis* from the periurethral skin, along the catheter surface, and into the bladder, thus initiating C-UTI. Hydrogel coatings appear to facilitate the migration of *P. mirabilis* over latex catheters. These coatings may therefore aid the colonization of the catheterized urinary tract by *P. mirabilis* and other uropathogenic bacteria.

ACKNOWLEDGMENTS

We thank Colin Hughes for providing the *flhA* mutant of *P. mirabilis* and George Payne for assistance in the isolation and analysis of transposon mutants. We are grateful to the Wellcome Trust, Beowulf

Genomics, and the Sanger Institute Pathogen Sequencing Unit for nucleotide sequence analysis of *P. mirabilis* strain HI4320.

REFERENCES

1. **Allison, C., L. Emody, N. Coleman, and C. Hughes.** 1994. The role of swarm cell differentiation and multicellular migration in the uropathogenicity of *Proteus mirabilis*. J. Infect. Dis. **169:**1155–1158.
2. **Allison, C., H. C. Lai, D. Gygi, and C. Hughes.** 1993. Cell differentiation of *Proteus mirabilis* is initiated by glutamine, a specific chemoattractant for swarming cells. Mol. Microbiol. **8:**53–60.
3. **Allison, C., H. C. Lai, and C. Hughes.** 1992. Co-ordinate expression of virulence genes during swarm-cell differentiation and population migration of *Proteus mirabilis*. Mol. Microbiol. **6:**1583–1591.
4. **Belas, R.** 1996. *Proteus mirabilis* swarmer cell differentiation and urinary tract infection, p. 271–293. *In* H. L. T. Mobley and J. W. Warren. (ed.), Urinary tract infections: molecular pathogenesis and clinical management. ASM Press, Washington, D.C.
5. **Cox, A. J., and D. W. Hukins.** 1989. Morphology of mineral deposits on encrusted urinary catheters investigated by scanning electron microscopy. J. Urol. **142:**1347–1350.
6. **Darouiche, R. O., H. Safar, and I. I. Raad.** 1997. In vitro efficacy of antimicrobial-coated bladder catheters in inhibiting bacterial migration along catheter surfaces. J. Infect. Dis. **176:**1109–1112.
7. **de Lorenzo, V., and K. N. Timmis.** 1994. Analysis and construction of stable phenotypes in gram-negative bacteria with Tn5- and Tn10-derived minitransposons. Methods Enzymol. **235:**386–405.
8. **Dufour, A., R. B. Furness, and C. Hughes.** 1998. Novel genes that upregulate the *Proteus mirabilis flhDC* master operon controlling flagellar biogenesis and swarming. Mol. Microbiol. **29:**741–751.
9. **Fraser, G. M., R. B. Furness, and C. Hughes.** 2000. Swarming migration by *Proteus* and related bacteria, p. 381–401. *In* Y. V. Brun and L. J. Shimkets (ed.), Prokaryotic development. ASM Press, Washington, D.C.
10. **Garibaldi, R. A., J. P. Burke, M. R. Britt, M. A. Miller, and C. B. Smith.** 1980. Meatal colonization and catheter-associated bacteriuria. N. Engl. J. Med. **303:**316–318.
11. **Gygi, D., G. Fraser, A. Dufour, and C. Hughes.** 1997. A motile but non-swarming mutant of *Proteus mirabilis* lacks FlgN, a facilitator of flagella filament assembly. Mol. Microbiol. **25:**597–604.
12. **Gygi, D., M. J. Bailey, C. Allison, and C. Hughes.** 1995. Requirement for FlhA in flagella assembly and swarm-cell differentiation by *Proteus mirabilis*. Mol. Microbiol. **15:**761–769.
13. **Hedelin, H., A. Eddeland, L. Larsson, S. Pettersson, and S. Ohman.** 1984. The composition of catheter encrustations, including the effects of allopurinol treatment. Br. J. Urol. **56:**250–254.
14. **Kanto, S., H. Okino, S. Aizawa, and S. Yamaguchi.** 1991. Amino acids responsible for flagellar shape are distributed in terminal regions of flagellin. J. Mol. Biol. **219:**471–480.
15. **Kirov, S. M., B. C. Tassell, A. B. Semmler, L. A. O'Donovan, A. A. Rabaan, and J. G. Shaw.** 2002. Lateral flagella and swarming motility in *Aeromonas* species. J. Bacteriol. **184:**547–555.
16. **Kunin C. M.** 1987. Detection, prevention and management of urinary tract infections, 4th edition, p. 245–288. Lea & Febiger, Philadelphia, Pa.
17. **Lewenza, S., B. Conway, E. P. Greenberg, and P. A. Sokol.** 1999. Quorum sensing in *Burkholderia cepacia*: identification of the LuxRI homologs CepRI. J. Bacteriol. **181:**748–756.
18. **Manoil, C.** 2000. Tagging exported proteins using *Escherichia coli* alkaline phosphatase gene fusions. Methods Enzymol. **326:**35–47.
19. **Mobley, H. L. T.** 1996. Virulence of *Proteus mirabilis*, p. 245–265. *In* H. L. T. Mobley and J. W. Warren (ed.), Urinary tract infections: molecular pathogenesis and clinical management. ASM Press, Washington, D.C.
20. **Morris, N. S., D. J. Stickler, and C. Winters.** 1997. Which indwelling urethral catheters resist encrustation by *Proteus mirabilis* biofilms? Br. J. Urol. **80:**58–63.
21. **O'Toole, G. A., and R. Kolter.** 1998. Flagellar and twitching motility are necessary for *Pseudomonas aeruginosa* biofilm development. Mol. Microbiol. **30:**295–304.
22. **Pratt, L. A., and R. Kolter.** 1998. Genetic analysis of *Escherichia coli* biofilm formation: roles of flagella, motility, chemotaxis, and type I pili. Mol. Microbiol. **30:**285–293.
23. **Romling, U., and M. Rhode.** 1999. Flagella modulate the multicellular behaviour of *Salmonella typhimurium* on the community level. FEMS Microbiol. Lett. **180:**91–102.
24. **Sabbuba, N., G. Hughes, and D. J. Stickler.** 2002. The migration of *Proteus mirabilis* and other urinary tract pathogens over Foley catheters. Br. J. Urol. **89:**55–60.
25. **Sambrook, J., E. F. Fritsch, and T. Maniatis.** 1989. Molecular cloning: a laboratory manual, 2nd ed. Cold Spring Harbor Press, Cold Spring Harbor, N.Y.
26. **Stamm, W. E.** 1991. Catheter-associated urinary tract infections: epidemiology, pathogenesis, and prevention. Am. J. Med. **91:**65S–71S.
27. **Stickler, D., and G. Hughes.** 1999. Ability of *Proteus mirabilis* to swarm over urethral catheters. Eur. J. Clin. Microbiol. Infect. Dis. **18:**206–208.
28. **Stickler, D. J., J. B. King, C. Winters, and S. L. Morris.** 1993. Blockage of urethral catheters by bacterial biofilms. J. Infect. **27:**133–135.
29. **Warren, J. W., L. Steinberg, J. R. Hebel, and J. H. Tenney.** 1989. The prevalence of urethral catheterization in Maryland nursing homes. Arch. Intern. Med. **149:**1535–1537.

Editor: J. B. Bliska